# Grid coupling by means of Chimera interpolation techniques

T. Schwarz and F. Spiering,
and N. Kroll
*DLR, Institute of Aerodynamics and Flow Technology, 38106 Braunschweig, Germany*

**Abstract**

**A coupling environment is presented which allows to couple two flow solvers with arbitrary spatial and temporal discretization. The design of the environment is described. The data exchange between the codes is based on Chimera interpolation techniques. The interpolation algorithms are generalized for interpolations close to curved surfaces in order to eliminate interpolation errors due to different surface discretizations. Flow simulations for a 2D NACA0012 airfoil and the aircraft configuration considered in the 4th AIAA Drag Prediction Workshopare are used to validate the method.**

## Nomenclature

| | |
|---|---|
| $d_1, d_2$ | distances |
| $s_1, s_2$ | scaling factors for distances |
| $w$ | weighting factor |
| $\vec{x}_P$ | coordinates of an interpolation point |
| $\vec{x}_{P*}$ | coordinates of a virtual interpolation point |
| $\vec{x}_S$ | coordinates of point on surface |
| $\vec{\varepsilon}$ | projection vector |

## 1 Introduction

At high angles of attack the nacelle of an airplane stalls and separated flow enters the fan of the engine. This situation is a challenging application for flow simulations by means of CFD methods, because the external flow around the aircraft and the nacelle must be simulated simultaneously with the internal flow when considering the fan. Several specialized CFD solvers are avaiable for external or turbomachinery flows, but most of them are not capable to simulate both disciplines at the same time. In order to enable such simulations coupling of two specialized CFD-solvers is necessary.

The coupling of two CFD-methods is not necessarily straight forward because of possibly differnt spatial or temporal discretizations, different solution algorithms and different programming languages Therefore, a dedicated coupling environment must be established which allows to control the two codes and enables a transfer of flow data between them.

Such a coupling environment is currently under development at DLR. This paper describes the lay-out of the coupling environment and the algorithms developed to transfer data between the codes. The long term goal ist to couple DLR's unstructured TAU solver for external flows with DLR's structured solver TRACE for turbomachinery flows. In the current state, only results for the TAU code are available.

In the current approach the two solvers will be coupled by means of the Chimera interpolation technique. This technique requires a certain overlap of the grid used to predict the external flow and the grid used to simulate the turbomachinery flow. For the application under consideration the overlap will be located at a certain distance in front of the fan inside the engine inlet, see Figure 1. The Chimera interpolation technique has the advantage that no

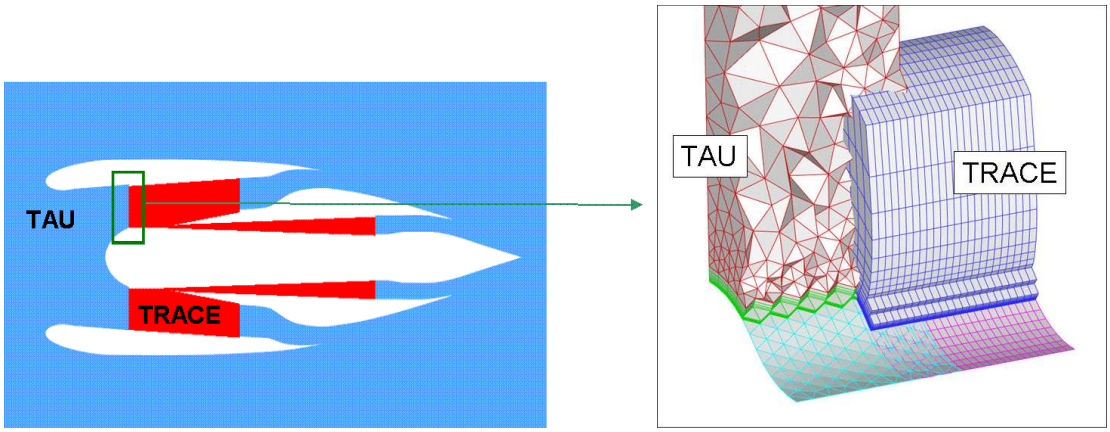


Figure 1: Envisaged coupling of TAU and TRACE

restrictions have to be applied on the grid topology and the grid point distributions in the overlap region. This is of high importance, because the TAU solver uses unstructured grids and a nodal based discretization whereas TRACE is based on structured grids and a cell centered discretization.

This paper is structured as follows: In Chapter 2 a brief introduction to the overset grid technique will be given. In Chapter 3 the coupling is environment described. For interpolation close to body surfaces the basic Chimera interpolation method has to be generalized, as described in Chapter 4. The new interpolation method will be applied to a 2D airfoil testcase and a 3D wing/body/horizontal-tail configuration in Chapter 5. The paper closes with a conclusion and an outlook.

# 2 Overset grid approach

The basis for the coupling environment are the interpolation procedures available with the Chimera approach. The Chimera technique or overset grid method introduced by Benek et al. [1] allows to assemble the computational grid by a collection of subgrids. The subgrids have a certain overlap with each other. At the outer boundaries of the subgrids flow data are interpolated from other grids, see Fig. 2. In most flow solvers tri-linear interpolation is applied. If some grid points of a subgrid fall inside a solid body, these points are flagged ('blanked') and excluded from the flow computations. The region of blanked points is called 'hole'. The hole creates an additional artificial boundary in the grid. The grid points at the fringe of the hole are also updated by interpolation.

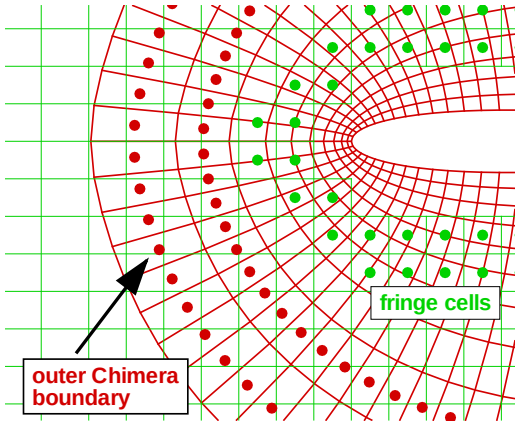


Figure 2: Sketch of two overset grids, interpolation points are marked with a dot

Since its invention the overset grid technique has been proven to be a reliable method for simulations involving rigid body motion, to simplify the grid generation process and to modify existing grids by adding additional grid components see for example, [2, 3].

# 3 Coupling environment

As briefly mentioned above, the coupling procedure has to take several requirements into account. The flow solvers TAU and TRACE are developed independently, so that the internal data structure and numerical algorithms are implemented differently. This implies the development of a coupling environment to perform the data exchange with minimized modifications of the flow solvers. Therefore the only modifications of the flow solvers are the implementation of a coupling boundary treatment and a data communication interface. The interpolation routines are implemented within the coupling environment.

Flow solvers usually run in parallel mode with multiple processes on a high performance computing system. Running two coupled flow solvers effectively is only possible if the major calculations are performed simultaneously. Furthermore efficient data communication between the coupling environment and the flow solvers is needed to preserve the scalability of the parallelization.

Therefore the coupling environment also uses parallel processes to provide a dedicated communication interface to each process of the flow solvers. This interface is realized by network socket communication whereas the internal data transfers of the coupling environment is realized by MPI (Message Passing Interface).

The coupling procedure incorporates the overset grid approach that is described above. The appliction of this method in the coupling environment can be divided into two major steps. In the first step appropriate interpolation source cells for each point of the coupling interface are searched for and the interpolation coefficients are calculated. In the second step the flow data is interpolated and exchanged between the flow solvers. Both steps are described in detail in the following sections.

## 3.1 Initialization

The first step shown in Fig. 3 initializes the coupling procedure and calculates the interpolation source points and the corresponding coefficients. After the computational grids and markers

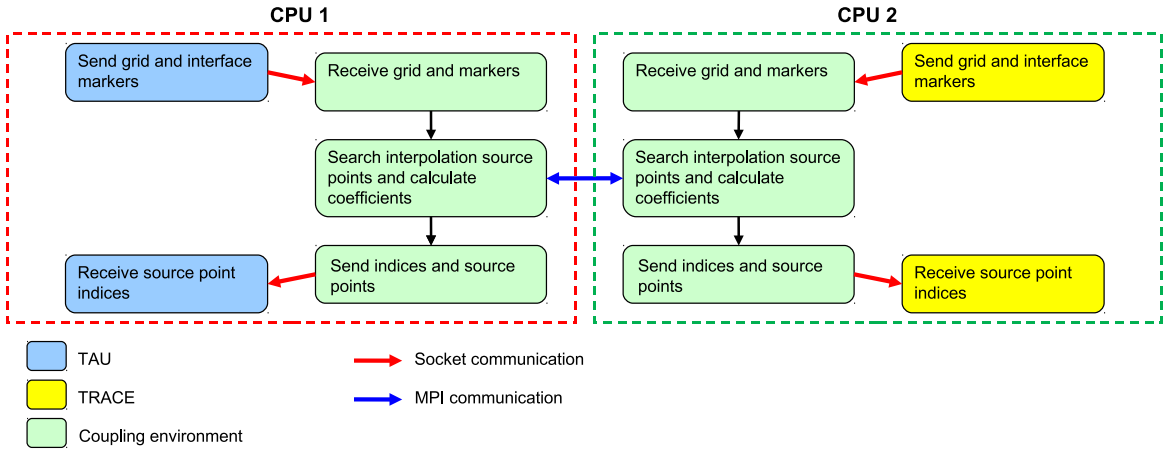


Figure 3: Calculation of interpolation coefficients

of the interface boundaries are transferred to the coupling environment, the appropriate grid partition of the opposing grid has to be searched for each interpolation target point. Then the coordinates of the target points are sent to the parallel process of the coupling environment that stores the appropriate source grid partition. Every parallel process then performs a local search for appropriate source cells for each received target point. These interpolation coefficients are stored in data structures within the coupling environment. Only the lists of the source point numbers are transferred back to the simulation codes.

This initialization step has to be performed only once for static grids. Only in case of moving grids or changes in the grid topologies the interpolation coefficients have to be recalculated.

### 3.2 Data Exchange

In the second step of the interpolation method the data is exchanged between the flow solvers, see Fig. 4. During the run of the flow solvers this step has to be performed every time step to provide a bidirectional coupling of the flow solution. At first the flow solvers send the flow data of the previously calculated interpolation source points to the coupling environment. After calculating the interpolated values, the data is exchanged between the parallel processes of the coupling environment to the parallel process of the coupling environment that holds the socket connection to the parallel process of the flow solver where the interpolated data is needed. After that the values of the interface boundaries are updated and the next iterative step of the flow solution is computed.

To synchronize the data exchange of the coupling procedure, the flow solvers have to stop in every iterative step of the flow solution. Therefore an appropriate balance of the computational times of both flow solvers is needed to reduce idle times of the computer system.

## 4 Grid overlap on body surfaces

### 4.1 Significance

In the foreseen application the grids for the two solvers will overlap a short distance ahead of the fan as shown in Figure 1. The overlap region is not only inside the flow but also touches the surfaces of the shaft and the nacelle. This requires an extension of the standard interpolation method because otherwise boundary layer data close to the surfaces would not

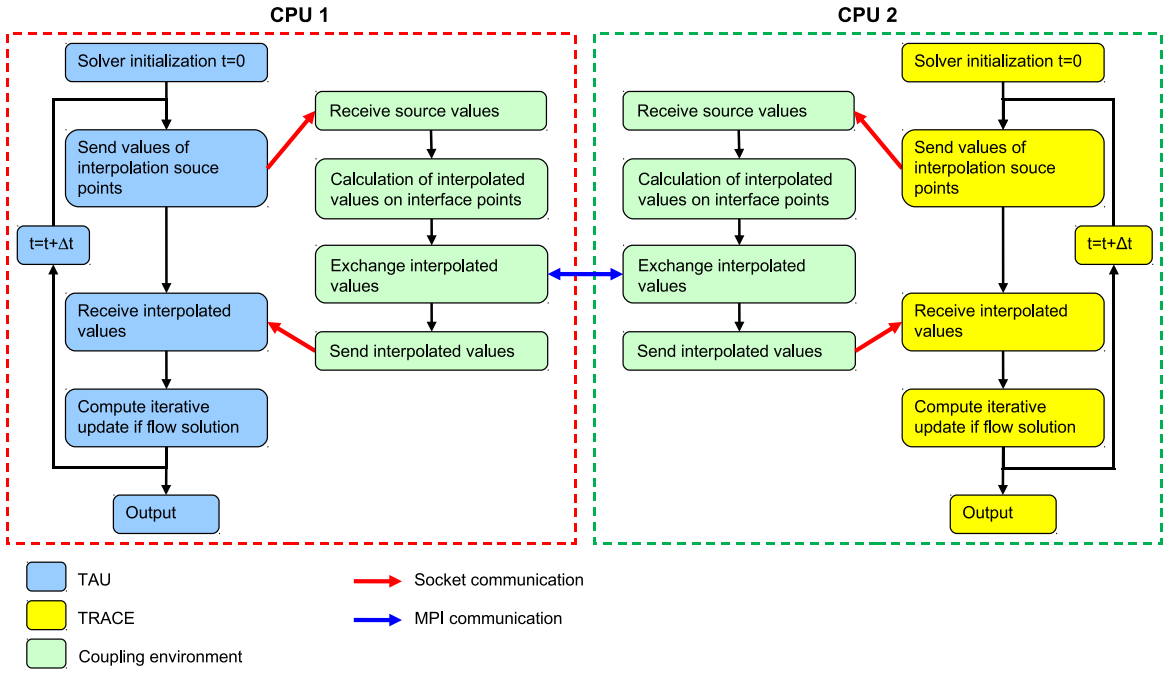


Figure 4: Flow data interpolation and exchange

be accurately interpolated. Although both grids cover the same surfaces in the overlap region, the discretizations of the surfaces are different because of the different grid point distributions. The different discretizations introduce errors in the interpolation coefficients and may even lead to a failure in the interpolation scheme. Figure 5, left shows the situation for a surface with convex curvature: For a given interpolation point $P$ the data are interpolated from an overset grid. The interpolated data will be inaccurate because the interpolation point has a wall distance $\delta_1$ which is different from the wall distance $\delta_2$ of the interpolated data. Due to the high velocity gradients inside boundary layer flows this interpolation error will significantly reduce the accuracy of the computed flow. For overlapping grids close to a concave surface

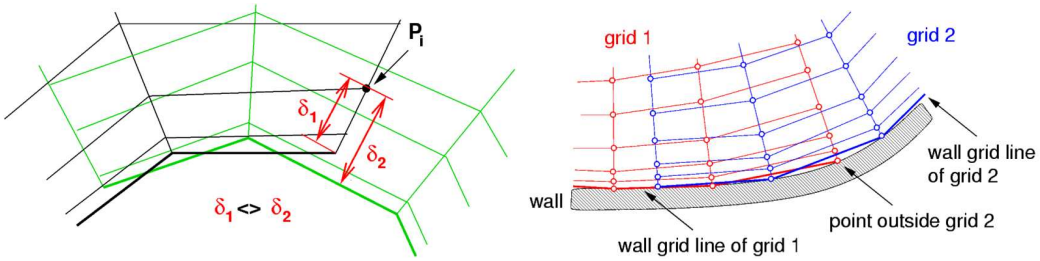


Figure 5: Invalid interpolation close to wall, left: wrong wall distance, right: point outside other domain

the same differences in wall distances can be observed, see Figure 5, right. Furthermore, some grid points near the wall may not be inside the overlapping grid, especially for Navier-Stokes grids with tiny grid spacing normal to the wall. The calculation of interpolation coefficients is therefore not possible for all points.

Several approaches are known in literature to solving the problem of interpolation close to surfaces. Noak and Belk [4] compute a transformation of coordinates based on the original CAD-geometry. Parks et al. [5] and Suhs et al. [6] modify the grid coordinates of the target

grid so that they are compliant with the donor grid. Another approach for the correction near surfaces has been developed by one of the authors of this paper [7, 8]. The method introduces the concept of a virtual target point. This approach has the advantages that 1) a CAD-surface is not required because the method is based on the grid coordinates, 2) the grid itself is not changed, and 3) the method can easily be parallelized. The method will be briefly described in the next section. A more detailed description including implementation issus for structured and unstructured solvers can be found in [9].

## 4.2 Projection algorithm

In order to correct the calculation of interpolation coefficients near surfaces a projection algorithm has been developed. For the explanation it is assumed that an interpolation point $P$ on grid $A$ interpolates data from grid $B$. The first step of the correction algorithm is to search grid $A$ for the point $P_S$ which is on a body surface and closest to the interpolation point $P$, see Figure 6, left. Next the point $P_S$ is projected onto the surface grid defined by the overlapping

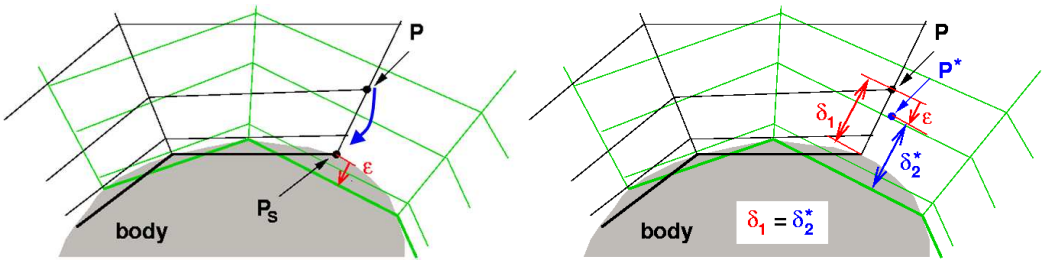


Figure 6: Projection method, left: projection of surface point $P_S$ which is closest to interpolation point P onto surface of overlapping mesh, right: calculation of virtual target point $P^*$

mesh $B$. The projection vector is denoted by $\vec{\varepsilon}$. In the third and final step of the projection method the projection vector $\vec{\varepsilon}$ is added to the coordinates $\vec{x}_P$ of the interpolation point. This gives the coordinates $\vec{x}_{P^*}$ of a virtual target point $P^*$, see Figure 6, right. The virtual target point $P^*$ has a wall distance $\delta_2^*$ which is identical to the wall distance $\delta_1$ of the original interpolation point.

The correction should be applied inside boundary layers only, whereas outside of boundary layers the original interpolation coordinates should be used. Therefore, the projection vector $\vec{\varepsilon}$ is scaled with a weighting factor $w$

$$\vec{x}_{P^*} = w \cdot \vec{\varepsilon} + \vec{x}_P \tag{1}$$

with

$$w = \begin{cases} 1 & \text{if } \vec{0} \leq |\vec{x}_P - \vec{x}_S| < d_1 \\ \frac{d_2 - |\vec{x}_P - \vec{x}_S|}{d_2 - d_1} & \text{if } d_1 \leq |\vec{x}_P - \vec{x}_S| < d_2 \\ 0 & \text{if } d_2 \leq |\vec{x}_P - \vec{x}_S| \end{cases} \tag{2}$$

Where $d_1$ and $d_2$ denote the range of wall distances for which full or no correction is to be applied.

Since the thickness of the boundary layer is not known a priori, the range of correction has to be calculated based on another measure. In this work the weight is calculated based on the length of the correction vector $\vec{\varepsilon}$.

$$d_1 = s_1 \cdot |\vec{\varepsilon}| \quad , \quad d_2 = s_2 \cdot |\vec{\varepsilon}| \tag{3}$$

To the authors' experience $s_1 = 10$ and $s_2 = 30$ give good results.

The coordinates of the virtual target point can now be used to calculate the interpolation coefficients. Because the wall distance is identical in both grids close to surfaces, the interpolated flow data will be accurate for arbitrarily bended surfaces. The projection algorithm for the correction of interpolation coefficients near surfaces will be presented in

# 5 Applications with improved Chimera interpolation

The improved interpolation near surfaces by using the projection method will be demonstrated by flow simulations with DLR's unstructured flow solver TAU [10]. TAU solves the RANS equations with a 2nd order finite volume discretization. For a detailed description of the wide range of available solution algorithms, turbulence models, etc. the reader is referred to the literature given above. The Chimera capabilities of TAU are described in [11].

## 5.1 NACA0012

The first test case is the flow about the NACA0012 airfoil. From the original C-type grid every grid line with an even index has been removed in circumferential direction. At the nose of the grid a Chimera hole was cut, see Figure 7. The hole is covered by a small local grid. It was extracted from the original grid and every grid line with an uneven index was removed. Figure 7, right illustrates the mismatch in the surface discretization of the two meshes. The flow was

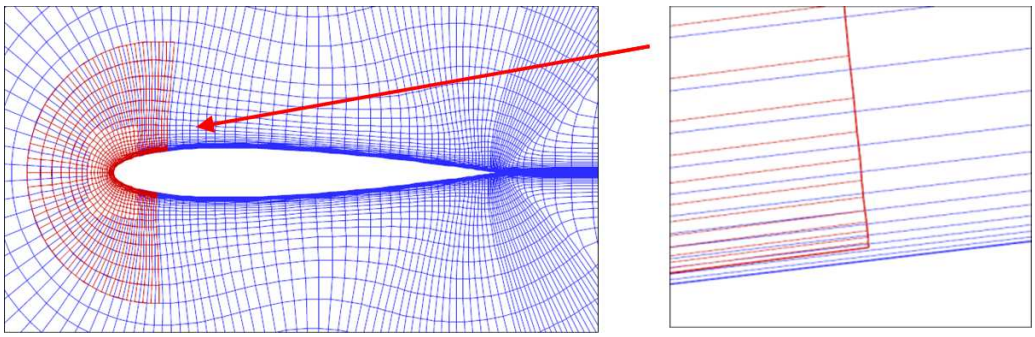

Figure 7: NACA0012 test case with mismatch of surface grid line at interpolation region

computed with the unstructured TAU solver for an inflow velocity of $M = 0.8$, an angle of attack $\alpha = 1.25^o$ and a Reynolds number of 4 million.

In Figure 8, left the results of the simulation without applying the projection method are compared to results on the grid for the profile without hole and overset grid. The pressure distributions compare well, whereas in the skin friction strong peaks can be seen in the interpolation area. In the boundary layer the pressure is almost constant normal to the wall whereas the velocity has a strong gradient. Therefore, the interpolation error has no effect on the pressure distribution but on the skin friction distribution. Applying the projection method for the correction of the interpolation coefficients gives correct results for the skin friction distribution, as shown in Figure 8, right. The results on the reference grid and the overset grid are nearly identical. The very small differences are caused by the different grid point distribution on the leading edge of the profile.

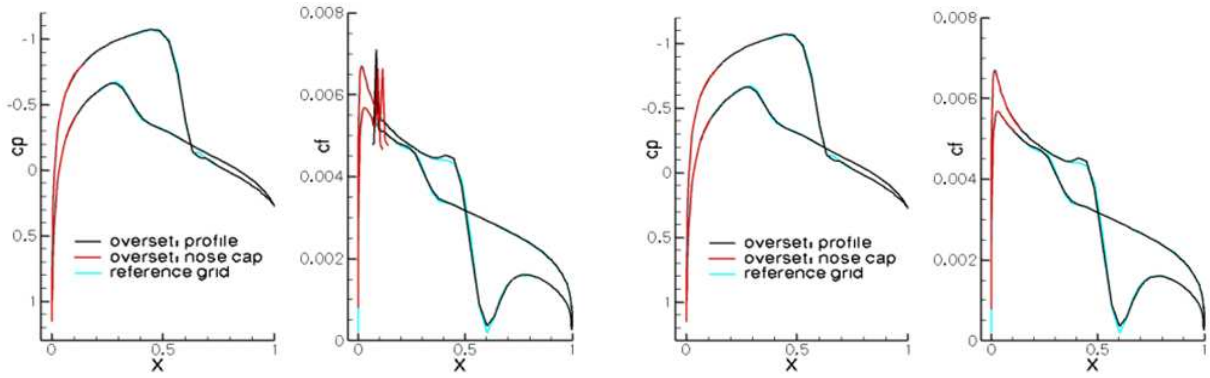


Figure 8: Pressure ($c_p$) and skin friction ($c_f$) distributions for simulation of NACA0012 test case, left: without wall-distance corrected interpolation, right: projection method applied

## 5.2 DPW4 aircraft configuration

A 3D test case is given by the aircraft configuration considered in the 4th AIAA Drag Prediction Workshop [12], see Figure 9, left. During the workshop the wing/body/horizontal-tail configuration is used to perform blind CFD simulations. Experimental data will be available in 2010. For the DPW4 configuration an unstructured grid was generated which has a poor

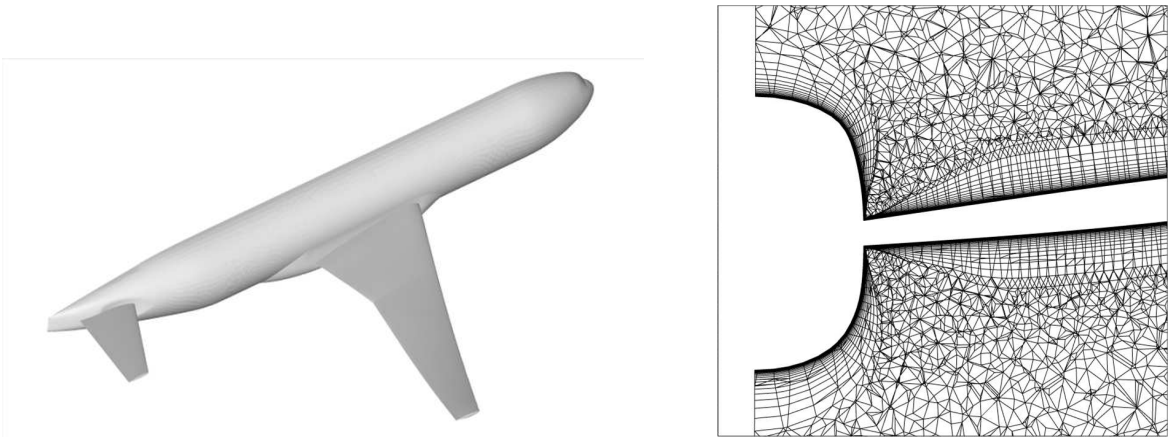

Figure 9: DPW4-configuration, left: configuration, right: grid slice showing poor boundary layer resolution at body/horizontal-tail junction

resolution of the boundary layer at the junction of the body and the horizontal tail plane, see Figure 9, right. This behavior is typical for unstructured grid generators. In order to improve the grid quality locally, a structured C-mesh was embedded into the main mesh, see Figure 10, left. The slice through the grid presented in Figure 10, right shows the good resolution of the boundary layer with the embedded grid. The additional grid adds 0.6 million grid nodes to the original grid with 11.6 million grid nodes.

The simulation was run for an inflow Mach number M=0.85, the angle of attack is $\alpha = 1^o$ and the Reynolds-number is five million. The resulting pressure and skin friction distributions are shown in Figure 11. The iso-pressure and iso-skin friction lines cross the Chimera interpolation boundaries smoothly.

The improvement in the boundary layer resulution is clearly visible in Figure 12, where on the original grid the downstream velocity component shows an unphysical kink at the junction

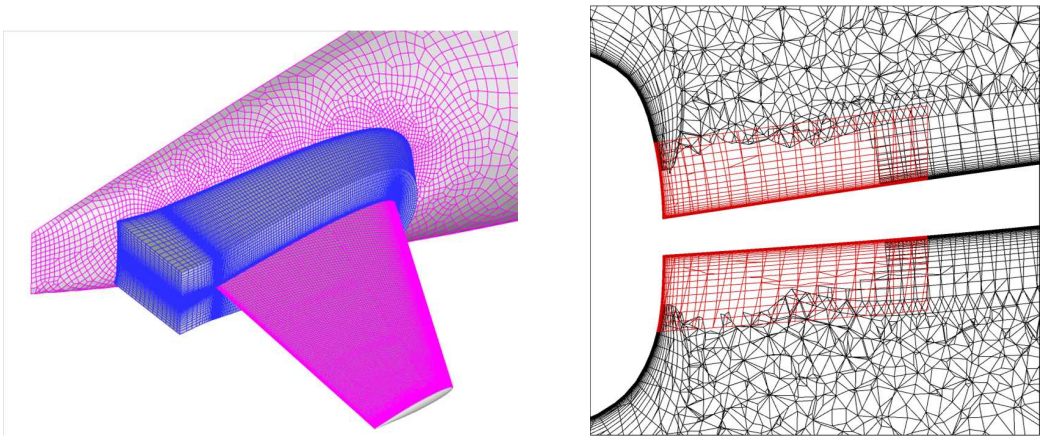

Figure 10: Structured mesh used to improve grid quality of original unstructured grid, left: overall view, right: slice through overset grid

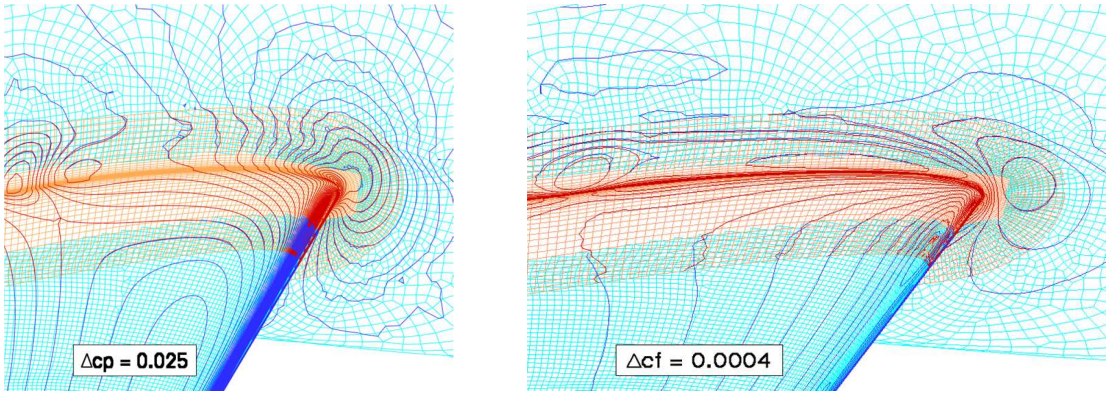


Figure 11: Pressure distribution (left) and skin friction distribution (right) at the body/horizontal-tail junction

of the body and the horizontal tail. In contrast, using the the overset grid gives the expected velocity profile of a corner flow.

As shown in Figure 13, left the boundary layer thickness simulated on the original mesh is significantly smaller than on the overset grid. This is due to the the very thin hexahedral sublayer in the mesh which is next to relatively coarse tetrahedral cells being much too coarse to accurately predict the boundary layer. The boundary layer is therefore artificially pressed into the thin sublayer which gives the inaccurate boundary layer profiles. As a consequence, the small separation predicted on the overset mesh is not visible on the original grid. This difference can also be seen by a comparison of the surface stream lines, see 13, right. The presence of the small separation at the trailing edge of the horizontal tail has to be confirmed by the wind tunnel experiment.

# 6 Conclusion

The numerical simulation of a stalling nacelle including the entry of the separated flow into the fan of the engine requires to couple specialized flow solvers for external and turbomachinery flows. The coupling method presented in this paper allows to couple any flow solvers on parallel computers. The coupling environment is based on Chimera interpolation algorithms allowing a

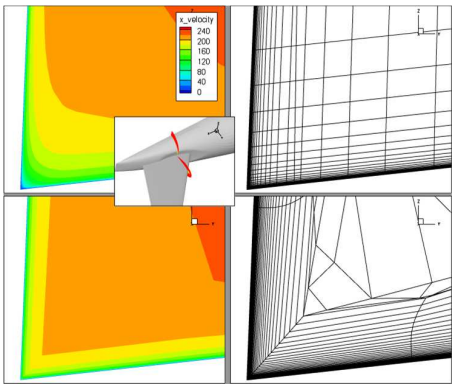

Figure 12: Downstream velocity componentThe projection algorithm for the correction of interpolation coefficients near surfaces will be presented in at the body/horizontal-tail junction, top: overset grid, bottom: original mesh

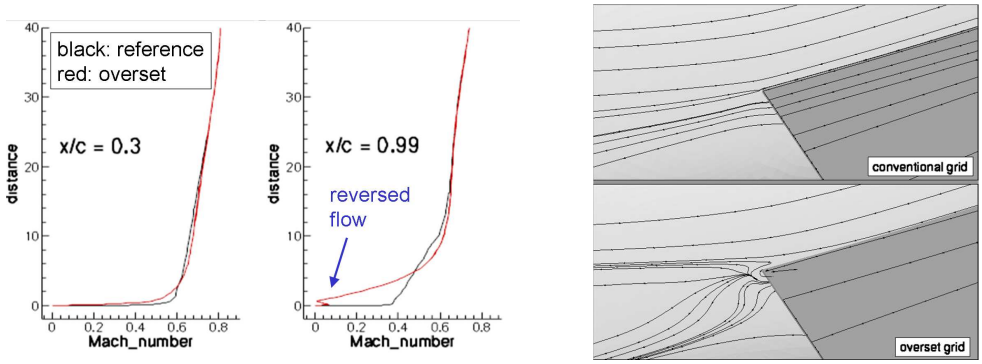


Figure 13: Flow near junction of horizontal tail plane and body, left: stream lines near trailing edge, right: boundary layer profiles

data exchange for any kind of mesh type and spatial discretization. Since the interpolation will be applied not only inside the flow field but also near body surfaces, a projection method has been developed which preserves the wall distances during interpolation. Without the correction the non-unique discretization of the body surfaces with two overlapping grids would introduce errors in the interpolated flow data. This would degenerate the quality of the boundary layers. The projection method has been implemented into the TAU solver. The elemination of the interpolation error is demonstrated for a flow simulation about an airfoil and a simulation of the flow about a wing/body/horizontal tail plane configuration.

Future work will concentrate on the development of the coupling environment. First applications will involve a coupling of DLR's structured turbomachinery code TRACE and DLR's unstructured code TAU for external flows. In addition, a tool for the the calculation of global forces and moments is under developent. In order to avoid double integration of surface loads in the overlap region a unique surface must be created. A method for structured grids is already available, see [8], which will be extended for unstructured grids.

# Acknowledgments

The members of the FOR 1066 research group gratefully acknowledge the support of the "Deutsche Forschungsgemeinschaft DFG" (German Research Foundation) which funded this

research.

# References


[1] Benek, J.; Steger, J. L.; Dougherty, F. C.: A Flexible Grid Embedding Technique with Application to the Euler Equations. AIAA Paper 83-1944, 1983

[2] Chan, W.M.: Overset grid technology development at NASA Ames Research Center. Computers and Fluids, Volume 3, Issue 3, March 2009

[3] Costes, M.; Pahlke, K.; D'Alascio, A.; Castellin, C.; Altmikus, A.: Overview of Results Obtained During the 6-Year French-German CHANCE Project. In: Proceedings of the American Helicopter Society 61st Annual Forum, Grapevine, USA, 01.-03. June 2005

[4] Noak, R. W.; Belk, D. M.: Improved Interpolation for Viscous Overset Grids. AIAA Paper 97-0199, 1997

[5] Parks, S. J.; Buning, P. G.; Steger, J. S.; Chan, W. M.: Collar Grids for Intersecting Geometric Components within the Chimera Overlapped Grid Scheme. AIAA Paper 91-1587, 1991

[6] Suhs, N. E.; Rogers, S. E.; Dietz, W. E.: PEGASUS 5: An Automated Pre-Processor for Overset-Grid CFD. AIAA Paper 2002-3186, 2002

[7] Schwarz, T.: Development of a Wall Treatment for Navier-Stokes Computations using the Overset-Grid Technique. In: Proceedings of the 26th European Rotorcraft Forum, The Hague, The Netherlands, 26. - 29. September, 2000

[8] Schwarz, T.: The Overlapping Grid Technique for the Time Accurate Simulation of Rotorcraft Flow. In: Proceedings of the 31st European Rotorcraft Forum, Florence, Italy, 13. - 15. September, 2005

[9] Schwarz, T.: An Interpolation Method Maintaining the Wall Distance for Structured and Unstructured Overset Grids. In: Proceedings of the CEAS 2009 European Air and Space Conference, Manchester, United Kingdom, 26. - 29. October, 2009

[10] Schwammborn, D.; Gerhold, T.; Heinrich, R.: The DLR TAU-Code: Recent Applications in Research and Industry. In: Proceedings of the European Conference on Computational Fluid Dynamics (ECCOMAS CFD 2006), Delft, The Netherlands, 5. - 8. September 2006

[11] Madrane, A.; Raichle, A.; Stürmer, A.: Parallel Implementation of a Dynamic Overset Unstructured Grid Approach. In: ECCOMAS 2004, Jyväskylä, Finland, 24.-28. July 2004

[12] Vassberg, J.C.; Dehaan, M.A.; Rivers, S.M.; Wahls, R.A.: Development of a Common Research Model for Applied CFD Validation Studies. AIAA-Paper 2008-6919, 2008